

Group 2 Artificial Muscles

Doctoral Assistant: Yegor Piskarev

Postdoctoral Researcher: Yi Sun

Mariane Brodier

Mst. Robotic Minor. Biomedical Technologies
Sciper: 250488

Théophile Balestrini

Ms. Robotic Minor. Space Technologies
Sciper: 306674

Christopher J. Stocker

Mst. Robotic Minor. IoT
Sciper: 266575

Abstract—The purpose of this report is to first outline the basic properties of dielectric elastomer actuator (DEA) as an effective method to provide large strains by transforming electrical energy into mechanical work. This is done in the form of a compliant capacitor. We tested this phenomenon on three differently sized frames (small, medium, large). These different frames allowed to test the effect of different prestrain on the film's ability to stretch and relax to different voltage potentials.

On a second term we looked at the models of electro-adhesion and characterization of adhesive performance relative to these models. The basic friction model is used to describe the critical shear force for a single electrode electro-adhesive. This electrode is made from conductive serpentine tape encased in parylene. The use of parylene results in thin dielectrics requiring high voltages (2.5 kV) to achieve shear force in the vicinity of 180 mN. We then also tested the effects of the surface roughness by scratching a piece of parylene with sandpaper and testing it against a normal smooth surface. The results showed that the scratched surface was able to sustain almost double the shear force than the normal smooth surface at 280 mN. We hypothesised that larger charge density could accumulate at the microscopic grooves made by scratching the surface. This larger charge density would reflect in a larger attraction between the surfaces resulting in a larger normal force [1].

Lastly we considered applying all the acquired knowledge to make a moving robot. We considered four different designs with different trades off between power and weight. We were able to successfully test three designs, with only one working remarkably well. Our circular design performed well by optimizing for power with the least amount of weight and by leveraging fast vibration like actuation that allowed it to displace forward when placed on a rough surface.

I. DEA CIRCLE ACTUATORS

Introduction

The purpose of the first part of the laboratory was to explore the effects of prestrain on **VHB 4905 acrylic elastomer**.

Theory

The working principle behind DEA is that of a compliant capacitor. An elastomeric film is coated on both sides with electrodes connected to a voltage. By applying a really high voltage the electrostatic pressure between the two electrodes compresses the elastomer film. This contracts the film thickness and expands it on the film's plane, thus flattening the film. When the circuit is opened the elastomer relaxes back to its original prestrained configuration. The electromechanical pressure of the material p_{eq} is equal to twice the electrostatic pressure p_{el} and is defined by:

$$p_{eq} = \epsilon_0 \epsilon_r \frac{U^2}{z^2} \quad (1)$$

The vacuum permittivity is denoted by ϵ_0 , the dielectric constant of the polymer by ϵ_r , the applied voltage U and the polymer thickness by z . The thickness of the **VHB 4905** is of 508 um. The polymer must have also high value of dielectric constant in order to be able to sustain the large load supplied on the electrodes. The material properties of the unstretched acrylic elastomer film are the following:

Acrylic elastomer film (unstretched) (3M, VHB4905)

| | |
|------------------------|--------------|
| Thickness | 508 um |
| Young's Modulus: | ~200-600 kPa |
| Relative Permittivity: | 4.68 |
| Breakdown Strength: | 24.8 V/um |

The changes in length in the x direction and y direction of our acrylic are shown below as well as their corresponding strain.

| | Δx [mm] | Δy [mm] | ϵ_x | ϵ_y |
|--------------|-----------------|-----------------|--------------|--------------|
| Small frame | 15 | 18 | 1.5 | 1.8 |
| Medium frame | 22 | 24 | 2.2 | 2.4 |
| Large frame | 30 | 32 | 3.0 | 3.2 |

Results

In order to analyze the effect of the electrical potentials on the different frame size we used an open-sourced program (*Kinovea*) to measure the change in diameter of the DEA in response to increasing intervals of electrode potential. This visual stretching of the DEA can be seen in the Figure 1. The top row showcases the small frames at different potentials followed by the medium frame and the large frame.

The results of the graph showed that the larger prestrain greatly contributed to larger stretching of the film under high voltage. The closer the two electrodes are together the higher the compression force and larger the electrical pressure [3]. This is an inverse quadratic relationship as outlined in the equation1.

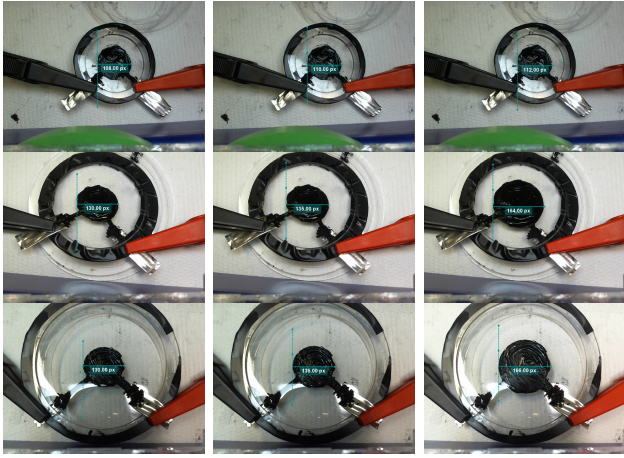


Fig. 1: DEA with different frame sizes at 0V , 1.4kV, and 3kV.

Figure 2 plots the different changes in diameter of the different frames in correspondence to different voltages.

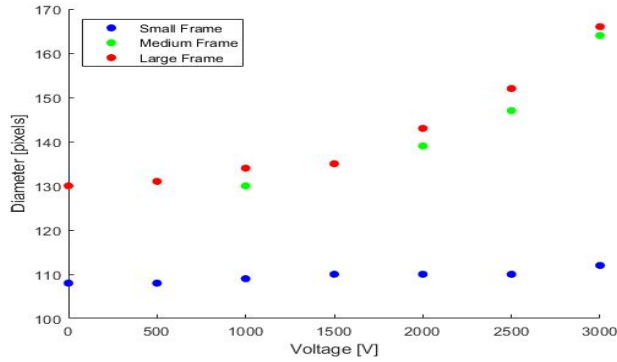


Fig. 2: Pixel Diameter versus Voltage plot

II. DEMES

Introduction

The purpose of the second part is to see the effect of changing frame stiffness of a DEMES device with constant DEA area.

Fabrication Procedure

In order to have a constant DEA area, all of the DEMES actuators are fabricated in the same way, only the frame will change. We used the circular frame as in the first part with 400% prestrain, and we made sure that all devices have near the same prestrain for comparison purposes.

The masks we used for this part are represented in figure 3. We observe that there are three different masks: what differentiates them is the width of the boundary between the area where we put the carbon grease and the extremities of the triangle.

We applied the carbon grease in the respective areas, and we connected the electrodes, as shown in figure 4.



Fig. 3: Triangle frames

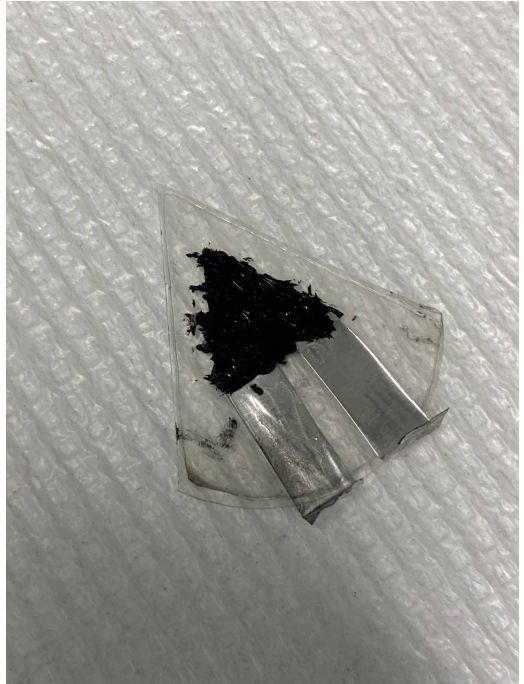


Fig. 4: DEMES device

In order to test the deflection movement of our devices, we used a LabView program that stepped through a predefined range of voltages and took a picture at each step.

Results

Figures 5 and 6 represent the result of the deflection movement. We used the mask with medium boundaries (placed on the middle of figure 3) for the experiment represented in figure 5, and we used the mask with large boundaries (placed on the right of figure 3) for the experiment represented in figure 6.

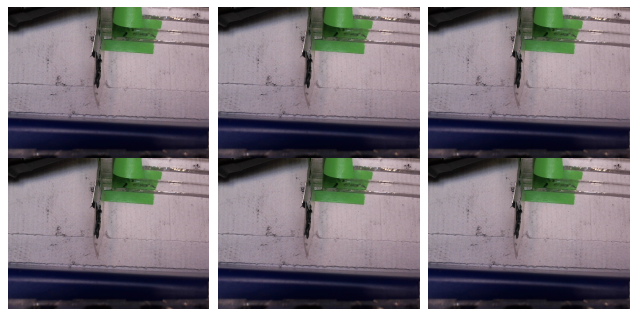


Fig. 5: DEMES with medium boundaries

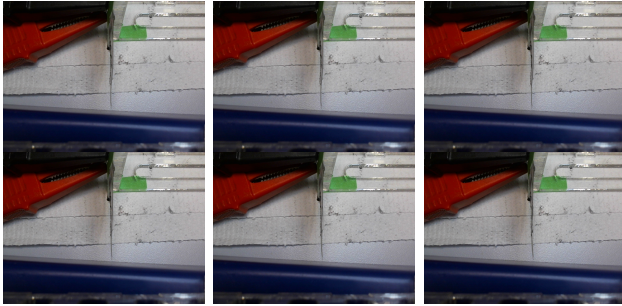


Fig. 6: DEMES with large boundaries

Here we focused on testing the effect of changing frame stiffness of a DEMES device with constant DEA area. We tracked the angle of deflection with the Kinovea app by measuring initial and final strain of each DEMES for the thin and medium frame as shown in Figure 7.

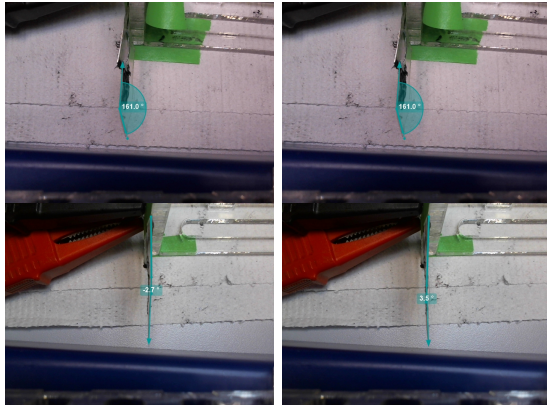


Fig. 7: DEA with different angle based on different frame shapes

On the medium frame we measured the acute angle as opposed to the obtuse but plotted the corresponding obtuse angle in Figure 8.

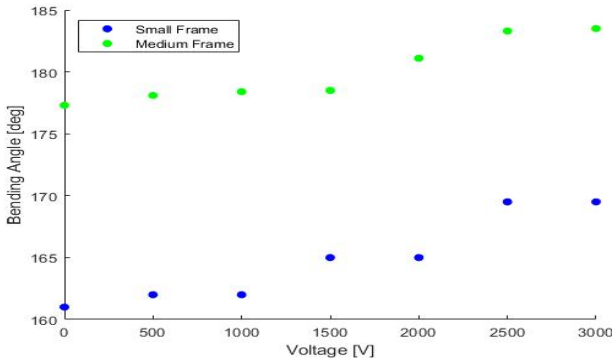


Fig. 8: Bending Angle versus Voltage plot

The plots don't show a very noticeable difference between the frames. This is very likely because we did not add enough prestrain to the film before adding the frame. A higher prestrain would give a better result for bending motion and angle deflection of the actuator. It is important to mention that

there is a sweet spot between pretension and actuation. Too much pretension and you may end up with a roll for electrodes which in turn could short-circuits the device. To little prestrain and the relaxed form does not change much from the actuated form. In our experiments we see that the frame with the small rim had a larger angle deflection than the medium with a thicker frame.

We observe that there is a higher deflection for the DEMES with medium boundaries. Unfortunately, we had some issues with the DEMES with small boundaries (placed on the left of figure 3), but we assume that if we could have tested it, it would have the highest deflection of the three masks. This is due to the fact that there is less area between the extremities of the triangle and the carbon grease, hence the device will be better able to bend.

In order to get an higher displacement, we must have the smallest boundaries, and the largest DEA. This will be demonstrated in the third part.

III. ROBOT

Introduction

The goal of this part is to use all the knowledge previously acquired to develop one or multiple robots that are capable of walking. Four different robots have been manufactured, all of them using DEMES devices. Three versions make use of one single DEA area and the objective is to make them crawl with the hypothesis that the friction coefficient with the ground will be different from one bending direction to the other. The third robot uses 4 DEMES devices mounted on a frame to form a quadruped. The objective is to make the robot walk by testing different gait sequences.

Fabrication Procedure

All DEA areas are manufactured in the same manner as the DEMES detailed in section II. A 20 mm x 20 mm square of VHB 4905 elastomer film is stretched across the largest frame, close to the maximum strain value of 300 % in order to get the maximum amount of deformation of the DEA when the device is in operation. Figure 9 shows all the PET films used as a semi-rigid frame to guide the device's deformation once the device is cut out of the annular frame it is mounted on.

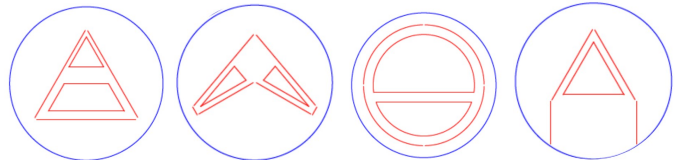


Fig. 9: DEA's geometries used for each robot

Figure 10 indicates how each DEA surface is prepared. The conductive carbon grease is applied over the green regions, on both sides, in order to form the capacitive electrodes. The dashed line represents the direction along which the DEA device should bend (following our interpretation of past results). From left to right, the three first devices (triangular, spearhead, and circular) are cut and used without further

modifications, the last one is cut and assembled on a PET frame for a total of four devices in order to obtain a quadruped.

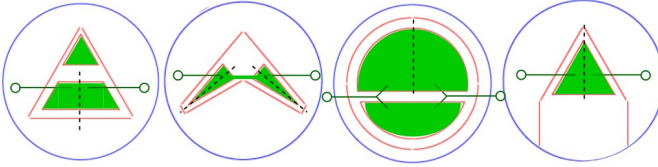


Fig. 10: Robots configuration, green areas are covered with carbon grease and dashed lines indicates the bending's direction. Green lines shows how the carbon electrodes are connected to the power supply, the two rings at their extremity represent for each device the (+) and (-) polarities

Figure 11 shows each device that are ready to operate once manufactured. The spearhead shaped device has finally not been manufactured because of its small size and the difficulty to shape it correctly.



Fig. 11: Finished robots, from left to right: triangular, circular, quadruped

Results

The actuation signal used to make the triangular and circular devices walk is the same, it is a square signal with a duty ratio of 0.5 and a frequency of 0.5 Hz. The chosen amplitude is 3 kV (Figure 12). Th triangular robot presented a good bending amplitude but the deformation was not able to make it move along a specific direction.

The circular robot presented an interesting behaviour: the two conductive layers of opposite polarity came sufficiently close to one another, when bending, to generate a discharge and come back into the initial state. As the process is cyclic when voltage is applied to the electrodes, it was occurring at a high frequency, in the range of hundreds of hertz. This behaviour allowed the robot to move forward at an impressive rate of a few millimeters per second. It is to note that such a behaviour was not planned in the design.

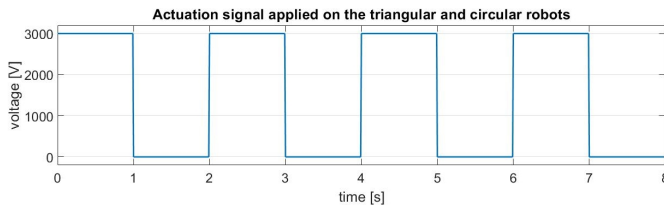


Fig. 12: Square signal with 3 kV amplitude and 0.5 duty-cycle injected in the DEA robots, triangular and circular shape.

The last experiment unfolded on the quadruped robot, which control signals were the same as the previous robots, but

alternated on each diagonal pair of legs. It means that when front-left and back-right legs where powered, front-right and back-left legs were unpowered, and vice-versa (Figure 13). Unfortunately, an issue was occurring with regards to the electrical connections and no actuation of any of the DEA devices has been observed.

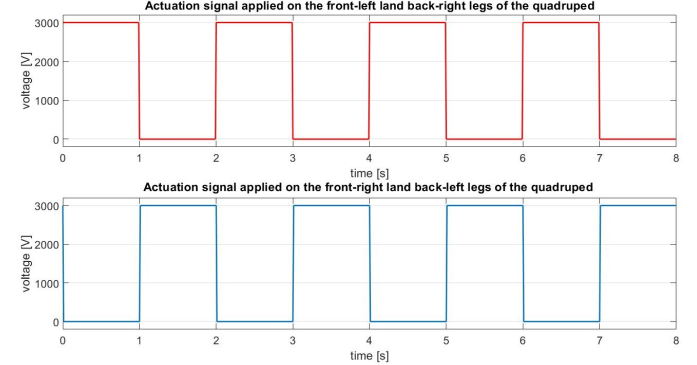


Fig. 13: Square signals with 3 kV amplitude and 0.5 duty-cycle injected in the DEA legs of the quadruped.

Improvements

One interesting approach could have been to stitch together multiple DEA devices and actuates them in such a sequence that the robot would have "rolled" on itself in order to move forward. On the other hand, this solution would have taken much more time and testing as it is rather complex. Thoughts have also been made on a very different system, where the DEA devices would serve as motors, providing power to more complex mechanical structure, e.g. using their traction force to pull on another system that would be defined as one or multiple legs (Figure 14). This solution is probably not feasible as such mechanical armature are generally heavy and the pulling force of the DEA actuator would not be sufficient to bear the structure's weight. A specific lightweight structure should be used or even additional PET film used in bending mode to mimic articulations of the leg.

IV. ELECTRODES

Introduction

The purpose of this part was to create an electrode in order to study the electroadhesion with kapton and paper.

Theory

Electroadhesion is an electrically controllable adhesion mechanism. It represents the electrostatic attraction between a conductor and a semiconductor when the two materials are in contact and a voltage is applied across them, creating an electrical potential difference between them. It is mainly used in fields such as robotic gripping, crawling and climbing, and active adhesion and attachment. It has been studied and used in fields including active adhesion and attachment, robotic gripping, robotic crawling and climbing, and haptics, for over a century. [2]

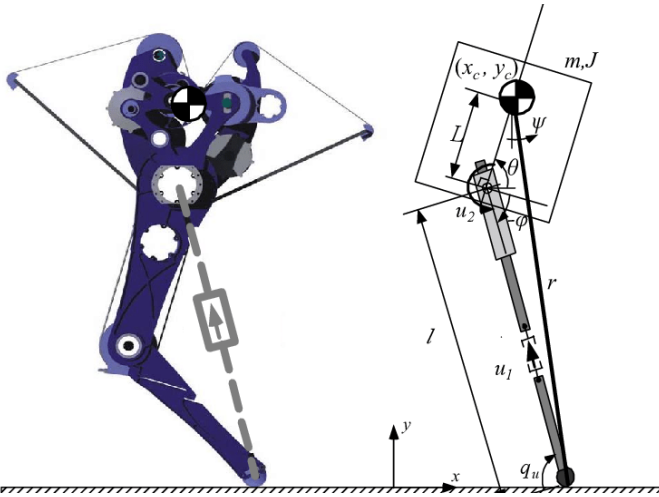


Fig. 14: Schematics of how a DEA device could actuate a leg.
(Source: <https://www.researchgate.net/profile/Ioannis-Poulakakis/publication/224296790>)

Fabrication Procedure

The EA pad consists of pairs of planar interdigitated electrodes embedded in a thin dielectric, as represented in figure 15. The dielectric material plays an important role in the adhesive action, but it also plays the role of a mechanical support for the electrodes. Moreover, it helps avoid dielectric breakdown and charge neutralization.



Fig. 15: Electrode

The conductors used for this experiment were kapton and a piece of paper. In figures 16 and 17 are shown the set up with kapton and a piece of paper respectively.

We also conducted the experiment with kapton scrubbed with sand paper. The difference in texture is observable in



Fig. 16: Setup with kapton



Fig. 17: Setup with paper

figure 18.

Results

In figure 19 is represented the mean value of load with respect with the applied voltage when using kapton. We observe that the curve trend is exponential, except at the value of 1500 V where there has been an issue during the experiment. The mean load value over the experiment was

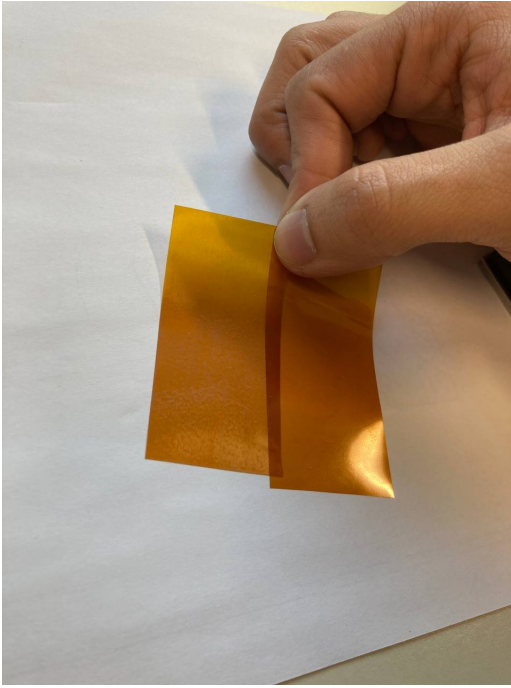


Fig. 18: Natural kapton vs kapton scrubbed with sand paper

0.012 N, so it is safe to assume that this threshold was exceeded around 1500 V.

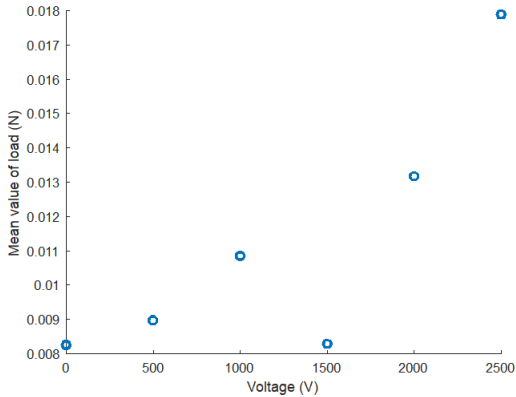


Fig. 19: Results with kapton

In figure 20 is represented the mean value of load with respect with the applied voltage when using kapton (in blue) and scrubbed kapton (in red). We wanted to observe if the texture of the material would provoke any changes. We observe that there was indeed a difference between the two textures: the scrubbed kapton has reached higher values in terms of load than for the non-scrubbed kapton. The curve trend is obviously still exponential, but the mean load value over the experiment was exceeded later for the scrubbed kapton (around 2000 V) than it was for the non-scrubbed kapton (around 1500 V).

In figure 21 is represented the mean value of load with respect with the applied voltage for paper. Here, the curve trend kind of follow an exponential trend, but begins to reach

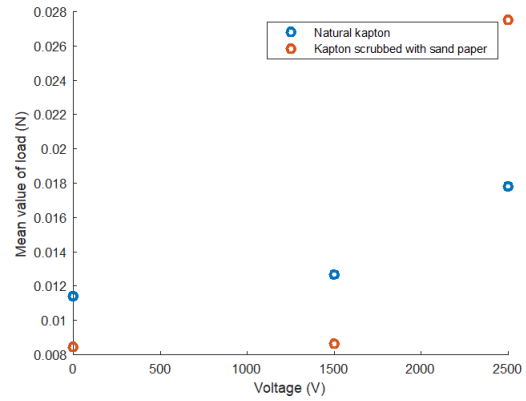


Fig. 20: Comparison between natural kapton and scrubbed kapton

a plateau at high voltage.

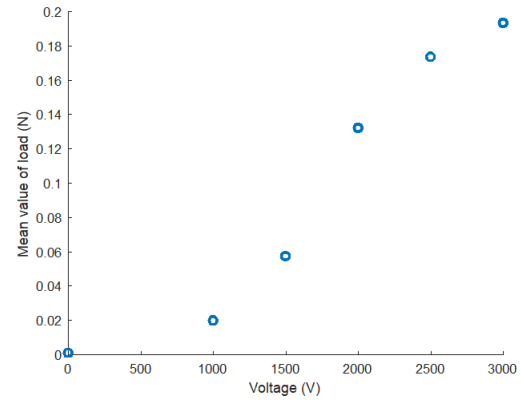


Fig. 21: Results with paper

V. ACKNOWLEDGEMENTS

We would like to thank the time and work of all the assistants brought to the three labs. Our group had great fun conducting the experiments and finishing winners of the robot race.

REFERENCES

- [1] Abraham Simpson Chen and Sarah Bergbreiter. A comparison of critical shear force in low-voltage, all-polymer electroadhesives to a basic friction model. *Smart Materials and Structures*, 26(2), 2017.
- [2] Jianglong Guo, Jinsong Leng, and Jonathan Rossiter. Electroadhesion Technologies for Robotics: A Comprehensive Review. *IEEE Transactions on Robotics*, 36(2):313–327, 2020.
- [3] Jun Shintake, Samuel Rosset, Bryan Schubert, Dario Floreano, and Herbert Shea. Versatile Soft Grippers with Intrinsic Electroadhesion Based on Multifunctional Polymer Actuators. *Advanced Materials*, 28(2):231–238, 2016.